Liquid jet leaping from a free surface

Jun Zou, Fangye Lin, Chen Ji, and Min Pan

Citation: Physics of Fluids **29**, 071702 (2017); doi: 10.1063/1.4994601
View online: http://dx.doi.org/10.1063/1.4994601
View Table of Contents: http://aip.scitation.org/toc/phf/29/7
Published by the American Institute of Physics

Liquid jet leaping from a free surface

Jun Zou,[1,a)] Fangye Lin,[1] Chen Ji,[1,a)] and Min Pan[2]
[1]*State Key Laboratory of Fluid Power and Mechatronic Systems, Zhejiang University, Hangzhou 310027, China*
[2]*Department of Mechanical Engineering, Center for Power Transmission and Motion Control, University of Bath, Bath BA2 7AY, United Kingdom*

(Received 4 February 2017; accepted 3 July 2017; published online 14 July 2017)

We investigate the characteristics of a liquid jet ejected from an inclined tube, which is submerged immediately under a free surface. Jets are classified into three regimes: the curtain regime, transition regime, and column regime. In all regimes, the jet trajectories deviate from the standard projectile function. An important reason is that additive liquid is entrained from the bulk. The capillary force also contributes to the deviation in the curtain regime. Models are established to predict the horizontal distance that a jet travels above the free surface in the curtain regime and column regime. *Published by AIP Publishing.* [http://dx.doi.org/10.1063/1.4994601]

Liquid jets are a classical topic that has been investigated for 100 years.[1] Liquid jets fall into two basic categories,[2] submerged jets and non-submerged jets, depending on whether the surrounding medium is the same as the medium of the jet. In the case of a typical non-submerged jet,[3–6] the liquid jet is ejected from a nozzle above the liquid surface into the air, and the trajectory, except for vertical ejection, can be roughly described by the parabolic curve $y = \frac{x}{v_0\cos\theta}\left(v_0\sin\theta - \frac{1}{2}g\frac{x}{v_0\cos\theta}\right)$, where y is the vertical displacement, x is the horizontal displacement, g is acceleration due to gravity, θ is the slant angle relative to the horizon, and v_0 is the average velocity of the liquid jet from the nozzle. In the case of a typical submerged jet,[1] the liquid jet is ejected from a nozzle below the liquid surface and does not leap out of the free surface. Submerged jets are widely used in underwater cleaning and cutting,[7] and many works therefore investigate their flow field and heat transfer.[8] Most previous studies on liquid jets focused on either a typical non-submerged jet (always traveling through air) or typical submerged jet (always traveling through water). In reality, however, it is not uncommon for liquid jets to emanate near but below the liquid surface. A fascinating example is the hunting method employed by the archerfish.[9–13] The fish ambushes insects from underwater and, like a sniper, shoots the insects down accurately with a liquid jet. Although the lips of the fish are sometimes above the water surface, there is certainly contact between the bulk liquid and the liquid in the mouth of the fish owing to the incomplete cheeks of the fish.[9–14]

In this letter, we explore the effect of a thin layer of liquid on the trajectory of a liquid jet submerged at a small depth. In addition, we establish a model to estimate the trajectory of the liquid jet leaping out of the liquid surface.

An experimental setup is developed to study the liquid jet leaping out of a free surface, as sketched in Fig. 1. A liquid jet is pumped out of a stainless-steel needle that is connected to a syringe via a small pipe. The syringe is pushed by an aluminum block that moves along a screw platform. A stepping motor is used to drive the block. In our experiments, the average velocity of the jet exiting the nozzle v_0 ranges from 1 to 4 m/s. The needle with inner radius $r = 0.65$ mm and outer radius $r' = 0.89$ mm is positioned underwater in a rectangular Plexiglas container ($15 \times 15 \times 60$ cm^3). The immerged depth γ, which is measured from the tip of the needle to the free surface, is 1.5–3.0 mm. The needle is first positioned at the free surface before it is moved to the target depth. To find the position of the free surface ($\gamma = 0$), the needle is first submerged and then lifted by a manual displacement platform until the tip of the needle approaches its mirror [Fig. 1(c)]. The resolution of the manual displacement platform is 0.01 mm. The slant angles of the needle θ range from 30° to 60°. The distance that the jet travels from the nozzle to the free surface is $c = \frac{\gamma}{\sin\theta} + \frac{r'}{\tan\theta}$. Two glycerin solutions are used as test fluids both in the tank and the syringe (Table I). For each experiment, the liquid in the syringe is the same as that in the bath. The experiments are carried out at atmospheric pressure, and the laboratory temperature is maintained at 20 ± 2 °C. The Reynolds number $\mathrm{Re} = \frac{2\rho v_0 r}{\mu}$ ranges from 100 to 1000. A clear boundary for liquid ejected from the needle [Figs. 2(c)–2(e)] is observed by adding red ink to the liquid inside the syringe.

To record the details of the jet behavior, a high-speed video camera (FASTCAM-ultima APX) fitted with a Nikkor 60-mm microlens is used.[15,16] Images are captured at 6000 frames per second. All the error bars in figures are obtained for three runs of experiments.

Typically, a jet is a stream of fluid that is projected into a surrounding medium. We therefore consider the jet under the free surface to be liquid ejected from the nozzle and the jet above the free surface to comprise all parts of the liquid medium. However, we only focus on the trajectory of the liquid ejected from the nozzle in this letter.

Two characteristic lengths of the jet intersecting with the free surface are shown in Fig. 2(a). l_1 denotes the length of the contact line between the jet and the bulk, while l_2 is the

a) Authors to whom correspondence should be addressed: junzou@zju.edu.cn and jich@zju.edu.cn

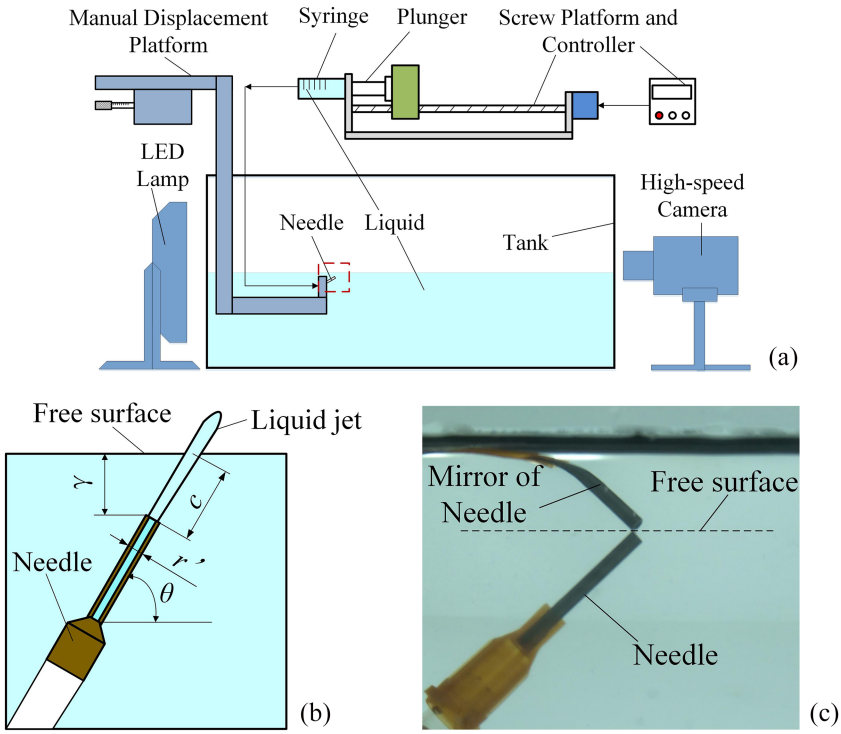

FIG. 1. Experimental setup. (a) Schematic diagram of the experimental setup. (b) Local enlarged drawing of the red square zone in (a). (c) Method used to find the plane of the free surface.

maximal horizontal distance that a jet travels above the free surface. For simplicity, we refer to l_1 and l_2 as the contact length and ejection length, respectively.

The evolution of contact lengths and ejection lengths for a jet with $\theta = 35^\circ$ and $\gamma = 2.0$ mm ($c = 4.76$ mm) is shown in Fig. 2(b). The liquid employed here is of type II. Generally, the jets can be divided into three regimes according to the two lengths [Figs. 2(c)–2(e)]: the curtain regime ($l_1 = l_2$), transition regime ($l_1 < l_2$ and $l_1 > 10r/\sin\theta$), and column regime ($l_1 < l_2$ and $l_1 \leqslant 10r/\sin\theta$). In the curtain regime, the jet above the free surface resembles a "liquid curtain" [Fig. 2(c)]. Both lengths (l_1 and l_2) extend as the jet velocity (v_0) increases. The jet enters a transition regime as the curtain collapses. In this regime, the contact length (l_1) retracts as the jet velocity (v_0) increases [Fig. 2(b)]. The jet continues to be curtain-like near the water-exit point and finally converges to a liquid column [Fig. 2(d)]. When the contact length (l_1) is close to its limit ($2r/\sin\theta$), the jet enters the column regime [Fig. 2(e)]. The division of the transition regime and column regime is set as $l_1 = 10r/\sin\theta$ in the present work.

For a standard projectile motion, the ejection length, $l_2 = v_0^2 \sin(2\theta)/g$, is drawn as a black line in Fig. 2(b). This equation well predicts the ejection lengths of the non-submerged liquid jet (black diamonds), which is totally surrounded by air. Unfortunately, it cannot be used to estimate the ejection length in all regimes here. We now explore the reasons for this.

Liquid is entrained from the bulk when the jet passes through the liquid layer. By adding red ink to the liquid inside the syringe [Figs. 2(c)–2(e)], we find that the jet above the free surface contains two parts: liquid from the syringe (red part) and liquid from the bulk (transparent part).

We thus explore how much liquid is entrained. A liquid jet with a total flow rate q_t above the free surface contains two parts: liquid from the syringe with a flow rate $q_0 = \pi r^2 v_0$ and liquid entrained from the bulk with a flow rate q_a. In our experiments, q_t can be calculated by measuring the total volume of the jet above the free surface in a certain period of time (see the supplementary material). It is noted that q_t is measurable only if the jet is in the transition regime or column regime. The analysis of the entrained liquid thus focuses on the column regime first. It is supposed that the total flow rate can be calculated by $q_t = \pi(r+h)^2 v_0$, where h is a length scale relative to the additive liquid. In our experiments, therefore, h can be calculated as $h = \sqrt{\frac{q_t}{\pi v_0}} - r$.

The experimental results [Fig. 3(a)] show that for a fixed slant angle ($\theta = 35^\circ$), increasing the characteristic length (c, by increasing γ) and the viscosity (μ) or decreasing the jet velocity (v_0) will increase h. Meanwhile, for jets with a constant characteristic length (c) but various slant angles (θ), h is indistinctive [Fig. 3(b)]. This may imply that the slant angle (θ) and the immerged depth (γ) affect the entrained liquid only through a change in the characteristic length (c). Furthermore, we found that h follows the scaling law $h = K\sqrt{\frac{\mu c}{\rho v_0}}$ [Fig. 3(c)]. The coefficient K obtained by fitting the experimental results is $K = 2.20$ for the type-I solution and $K = 2.45$ for the type-II solution.[19]

TABLE I. Properties of glycerin solutions.

Glycerin solution	Density ρ (kg/m^3)	Viscosity μ (mPa s)	Surface tension σ (N/m)
Type I	1155	4.5	0.063
Type II	1166	7.5	0.061

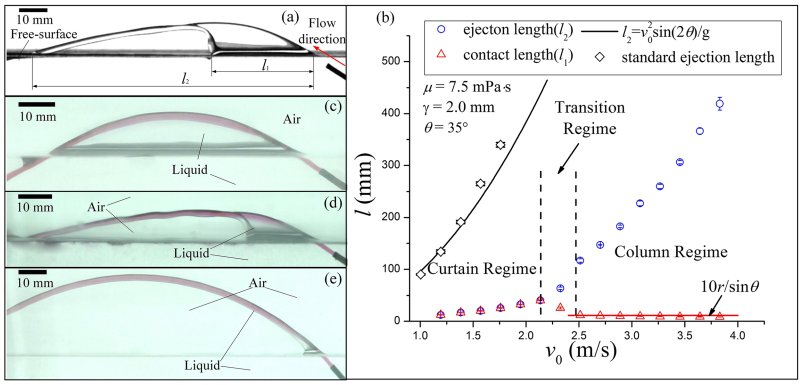

FIG. 2. Phenomena of liquid jet leaping from the free surface. (a) Schematic diagram of the contact length and ejection length. (b) Development of the contact length l_1 (red triangles) and ejection length l_2 (blue circles) with an increase in jet velocity (v_0) under the experimental conditions $\theta = 35°$ and $\gamma = 2$ mm ($c = 4.76$ mm). The glycerin solution used here was of type II. Black diamonds denote to a standard ejection length (the ejection of a jet in air), which can be estimated according to $l_2 = v_0^2 \sin(2\theta)/g$ (black line). (c) Curtain regime. (d) Transition regime. (e) Column regime. The division between the transition regime and column regime is set as $l_1 = 10r/\sin\theta$.

In the case of a high-speed solid column passing through a liquid bulk, it has been found that the liquid entrained in the volume is a viscous boundary layer.[17–20] The maximum thickness δ of the boundary layer follows the scaling law $\delta \sim \sqrt{\frac{\mu c}{\rho v_0}}$. So if this scaling law is also available for the boundary layer of liquid columns, it may imply that the length scale of the additive liquid is relative to the maximum thickness of the boundary layer: $h \sim \delta$.

The liquid entrained by the boundary layer causes the slowdown of the jet and finally induces the deviation of the jet trajectory. For a jet in the column regime, it can be assumed that the entrained liquid has the same velocity as the liquid from the needle above the free surface [Fig. 2(e)]. Then, according to momentum conservation, the equivalent average velocity of the liquid jet v_1 at the water-exit point follows the rule $q_t v_1 = q_0 v_0$. The equivalent jet velocity v_1 of the jet in the column

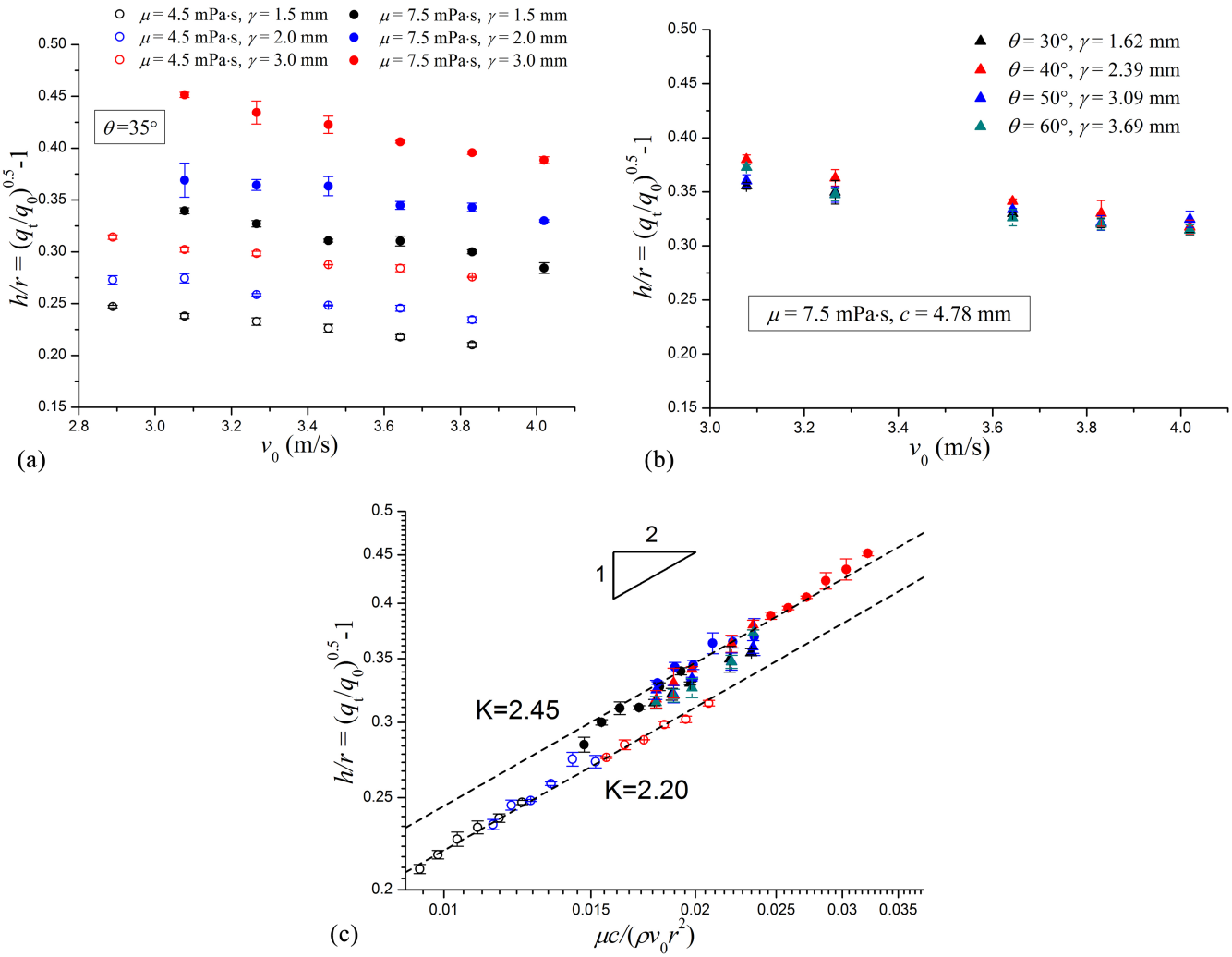

FIG. 3. Quantity of the entrained liquid. (a) h with varying immerged depth and liquid viscosity. (b) h with constant characteristic length but varying immerged depth and slant angle. (c) Scaling law for h. The symbols in (c) match those in (a) and (b). All data are for a jet in the column regime.

regime is therefore

$$v_1 = \frac{1}{(1+h/r)^2} v_0. \quad (1)$$

The momentum transfer is complex in the curtain regime. Although the development of the boundary layer is independent of γ and the jet morphology over the free surface (i.e., a curtain or column), it is difficult to determine whether $h = K\sqrt{\frac{\mu c}{\rho v_0}}$ still holds. Additionally, for a jet in the curtain regime, there is an appreciable velocity gradient in the curtain, which means that the average efficient velocity of the entrained liquid may be lower than the velocity of the liquid from the needle (see the supplementary material). For the curtain regime, therefore, considering both the velocity distribution in the curtain and the uncertainty of the flow rate of the entrained liquid, a coefficient k is used to modify the momentum of the entrained liquid: $q_0 v_1 + k q_a v_1 = q_0 v_0$. The equivalent jet velocity v_1 for a jet in the curtain regime is

$$v_1 = \frac{1}{k(1+h/r)^2 + 1 - k} v_0. \quad (2)$$

The jet morphology above the free surface in the column regime is similar to that in the standard liquid-jet case. In these two cases, the gravity force and inertial force dominate the jet motion. The jet in the column regime is therefore regarded as a standard liquid jet with initial velocity v_1. The ejection length for a jet in the column regime can thus be calculated as

$$l_2 = \frac{\sin 2\theta}{g} v_1^2. \quad (3)$$

By combining Eqs. (1) and (3), the ejection length for a jet in regime I can be predicted. Figure 4(a) shows that Eq. (3) can well predict the ejection length with varying viscosity and characteristic length.

For a jet in the curtain regime, the liquid curtain is regarded as a liquid sheet that connects a liquid column and the bulk (see the supplementary material). In other words, the liquid column is dragged downward by the liquid sheet (under a capillary force). The magnitude of viscous and gravitational forces relative to the capillary force is prescribed by the Ohnesorge number $Oh = \frac{\mu}{\sqrt{\sigma r \rho}}$ and the bond number $Bo = \frac{\rho g r^2}{\sigma}$, respectively; $Oh \sim 0.01$ and $Bo \sim 0.1$. Therefore, although both the capillary force and the gravity force drag the jet downward, it is reasonable to ignore the gravity in the curtain regime. As the capillary force remains perpendicular to the jet rim, the jet trajectory can be regarded as circular motion. The ejection length for a jet in the curtain regime is

$$l_2 = \frac{\rho \pi r^2 \sin\theta}{\sigma} v_1^2. \quad (4)$$

By combining Eqs. (2) and (4), the ejection length for a jet in the curtain regime can be predicted. Figure 4(b) shows that our model can well predict the ejection length with varying viscosity and characteristic length. Here, the coefficient k is fitted as 0.28 using Eq. (2), which implies that jets in the curtain regime with varying velocity and slant angle may have similar distributions of the velocity field in the volume.

A jet in the transition regime is indeed in a transition state between the curtain regime and column regime. Its trajectory is a composition of circular motion and projectile motion. However, it is difficult to predict the ejection length unless the contact length can be predicted.

We investigated the characteristics of a liquid jet ejected from an inclined nozzle, which is submerged by a thin layer of liquid. There are three regimes according to the jet morphology above the free surface: the curtain regime, transition regime, and column regime. In all regimes, the jet trajectory deviates from the standard projectile function. An important reason is that an additive liquid is entrained from the bulk when the jet passes through the thin layer of liquid. It was found that the length scale h relative to the additive liquid follows the scaling law $h = K\sqrt{\frac{\mu c}{\rho v_0}}$ in the column regime. The equivalent average velocity for a liquid jet v_1 was estimated according to the momentum conservation for the curtain regime and column regime. Finally, models were established to predict the ejection length.

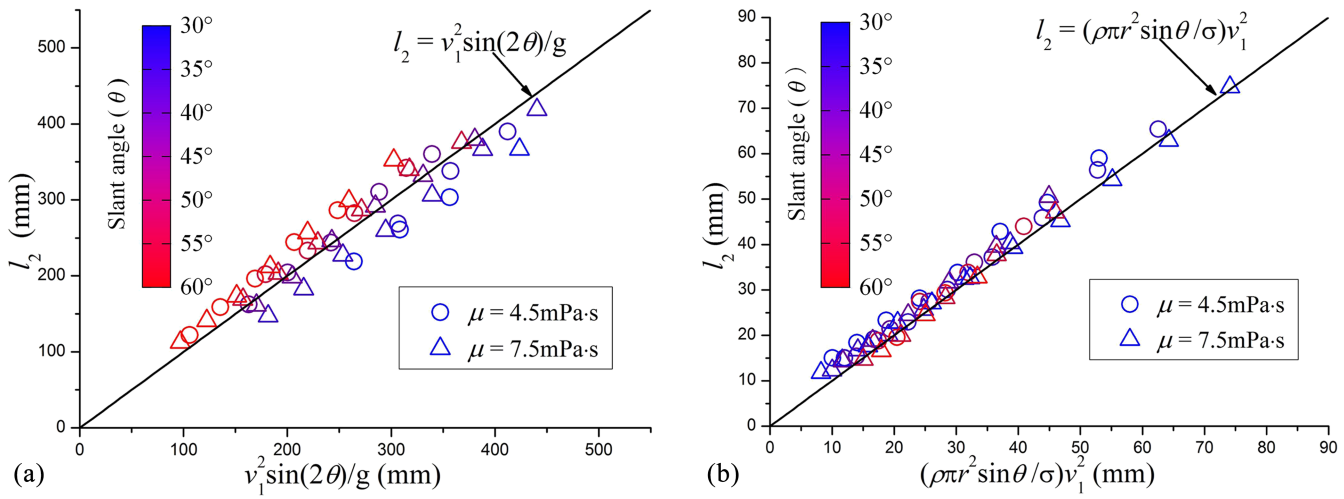

FIG. 4. Ejection length for liquid jets with varying slant angles (θ) of 30°–60°: (a) column regime and (b) curtain regime. The immerged depth (γ) is fixed at 2.0 mm. The characteristic length (c) varies from 2.8 to 5.5 mm. The solid line is the theoretical value predicted by our model, as described by Eqs. (4) and (5). Triangles give results for the glycerin solution of type I and circles give results for the glycerin solution of type II.

See supplementary material for more details, showing the measurement of total jet flow rate (q_t), the flow field in the curtain regime, and the model for the jet trajectory in the curtain regime.

This work is supported by the National Natural Science Foundation (Nos. 51475415, 51405429, and 51521064), Zhejiang Provincial Natural Science Foundation for Distinguished Young Scholars (No. LR15E050001), and Research Project of the State Key Laboratory of Mechanical System and Vibration (Grant No. MSV201706).

[1] J. Eggers and E. Villermaux, "Physics of liquid jets," Rep. Prog. Phys. **71**(3), 036601 (2008).
[2] N. Nitin, "Transport phenomenon in jet impingement baking," Ph.D. dissertation (The State University of New Jersey, 2009).
[3] J. E. Goff and C. Liyanage, "Projectile motion gets the hose," Phys. Teach. **49**, 432 (2011).
[4] F. Celestini, R. Kofman, X. Noblin, and M. Pellegrin, "Water jet rebounds on hydrophobic surfaces: A first step to jet micro-fluidics," Soft Matter **6**, 5872 (2010).
[5] M. Li, A. Saha, D. L. Zhu, C. Sun, and C. K. Law, "Dynamics of bouncing-versus-merging response in jet collision," Phys. Rev. E **92**, 023024 (2015).
[6] J. W. M. Bush and A. E. Hasha, "On the collision of laminar jets: Fluid chains and fishbones," J. Fluid Mech. **511**, 285 (2004).
[7] A. Guha, R. M. Barron, and R. Balachandar, "An experimental and numerical study of water jet cleaning process," J. Mater. Process. Technol. **211**, 610 (2011).
[8] K. P. Judd, I. Savelyev, Q. Zhang, and R. A. Handler, "The thermal signature of a submerged jet impacting normal to a free surface," J. Visualization **19**, 1 (2016).
[9] M. Ben-Tov, O. Donchin, O. Ben-Shahar, and R. Segev, "Pop-out in visual search of moving targets in the archer fish," Nat. Commun. **6**, 6476 (2015).
[10] A. Vailati, L. Zinnato, and R. Cerbino, "How archer fish achieve a powerful impact: Hydrodynamic instability of a pulsed jet in toxotes jaculatrix," PLoS One **7**, e47867 (2012).
[11] P. Gerullis and S. Schuster, "Archerfish actively control the hydrodynamics of their jets," Curr. Biol. **24**, 2156 (2014).
[12] S. Temple, N. S. Hart, N. J. Marshall, and S. P. Collin, "A spitting image: Specializations in archerfish eyes for vision at the interface between air and water," Proc. R. Soc. B **277**, 2607 (2010).
[13] L. M. Dill, "Retraction and the spitting behavior of the archerfish (Toxotes chatareus)," Behav. Ecol. Sociobiology **2**, 169 (1977).
[14] W. Kim and J. W. M. Bush, "Natural drinking strategies," J. Fluid Mech. **705**, 7 (2012).
[15] J. Zou, P. F. Wang, T. R. Zhang, X. Fu, and X. D. Ruan, "Experimental study of a drop bouncing on a liquid surface," Phys. Fluids **23**, 044101 (2011).
[16] L. Hu, M. B. Li, W. Y. Chen, H. B. Xie, and X. Fu, "Bubbling behaviors induced by gas-liquid mixture permeating through a porous medium," Phys. Fluids **28**, 087102 (2016).
[17] A. De Ryck and D. Quere, "Inertial coating of a fiber," J. Fluid Mech. **311**, 219 (1996).
[18] D. Quere, "Fluid coating on a fiber," Annu. Rev. Fluid Mech. **31**, 347 (1999).
[19] E. Ruckenstein, "Transport phenomenon in jet impingement baking," J. Colloid. Interface Sci. **246**, 393 (2002).
[20] S. Rebouillata, B. Ste-eninoa, and B. Salvador, "Hydrodynamics of high-speed fibre impregnation: The fluid layer formation from the meniscus region," Chem. Eng. Sci. **57**, 3953 (2002).